Journal of the European Ceramic Society 19 (1999) 329–334

PII: S0955-2219(98)00164-2
0955-2219/99/$—see front matter

Simulation of Crack Propagation in Alumina Particle-dispersed SiC Composites

Marc-Oliver Nandy,[a] Siegfried Schmauder,[a]* Byung-Nam Kim,[b] Makoto Watanabe[b] and Teruo Kishi[b]

[a]Staatliche Materialprüfungsanstalt, University of Stuttgart, Pfaffenwaldring 32, 70569 Stuttgart, Germany
[b]Research Center for Advanced Science and Technology, The University of Tokyo, 4-6-1 Komaba, Meguro-ku, Tokyo 153, Japan

(Received 15 October 1997; revised version received 28 April 1998; accepted 16 June 1998)

Abstract

Addition of alumina particles to silicon carbide results in strongly improved toughness values. In order to come to a better understanding of this phenomenon, crack propagation is simulated for a 20 vol% alumina particles-dispersed silicon carbide composite material using the Body Force Method. Special emphasis is paid to the influence of graded compositions. Numerically obtained crack paths are compared to crack paths generated experimentally by Vickers indentations. Moreover, mechanical properties of the investigated material were measured experimentally. Microstructural toughness variations as well as the direction of crack propagation are found to be strongly influenced by residual stresses due to the mismatch between thermal expansion coefficients of alumina and silicon carbide and by the actual crack location. According to tensile residual stresses in the radial direction cracks approaching a particle are deviated circumferentially in the matrix around the particle. Moreover, the failure behavior of cracks propagating into a zone of increasing or decreasing volume fraction of alumina particles is found to behave differently as residual stress fields superimpose in the case of particle clustering. © *1999 Elsevier Science Limited. All rights reserved.*

Keywords: composites, SiC, Al_2O_3, crack propagation, mechanical properties, simulation.

1 Introduction

Recently, several crack path simulations in two-dimensional polycrystals and particle-dispersed composites have been performed using the body force method.[1,2] Kim *et al.* have shown how a crack in a particle-dispersed ceramic composite interacts with the particles. In a material with SiC matrix and 10 vol% randomly dispersed Al_2O_3 particles the crack propagated between the particles being repelled by circumferential thermal residual stresses in the matrix around the particles. The related fracture resistance increased when the crack was approaching a particle and decreased remarkably when the crack had passed it. In contradiction with many experimental results[3] the overall fracture resistance with crack extension was lower than the initial crack resistance value of the matrix which was related to the lack of important 3D-toughening mechanisms in this 2D simulation.

In the present study, simulated crack paths are compared to experimental results. The object of these investigations is a SiC matrix containing 20 vol% randomly dispersed alumina particles. The mechanical properties such as 4-point-bending strength and fracture toughness were determined experimentally for monolithic SiC as well as for the composite. The fracture toughness of the monolithic material was used as the K_{IC} value of the matrix in the simulation. The particles are assumed to remain intact in agreement with experimental findings.[4] The fracture resistance values derived from the simulation were then compared to the experimentally obtained fracture toughness of the composite material.

Additionally, crack paths were simulated in a material with increasing or decreasing volume fraction of alumina particles in the direction of crack propagation, respectively. The fracture resistance in such compositionally graded materials is calculated as a function of crack extension.

2 Methods

2.1 Mechanical properties

The monolithic SiC ceramic as well as the composite material containing 20 vol% Al_2O_3 particles

*To whom correspondence should be addressed.

(SiC/Al_2O_3 (20 vol%)$_p$) were processed by hot-pressing the mixed powders for 6 h at 2000°C.[4] Relative densities were measured using the Archimedes technique. The hot pressed bodies were cut into beam shaped specimen of 3 by 4 by 40 mm. The prospective tensile surfaces were polished to a 1 μm finish, and the tensile edges were chamfered to reduce stress concentrations.

In order to determine the bending strength, seven specimens were fractured in four-point bending (inner span: 10 mm, outer span: 30 mm) at room temperature for each material using a universal testing machine at a crosshead speed of 0·5 mm min^{-1}. Failure loads were measured with a calibrated load cell, and the bending strength values were calculated from the conventional beam formula.

Fracture toughness was determined by applying the Single Edge Precracked Beam (SEPB) method[5] for five specimens each.

In order to analyze the crack propagation modes in the composite material, Vickers indentations were placed on the polished surfaces of the specimens. The cracks which originated from the edges of these indentations were examined by an optical microscope (OM).

2.2 Simulation of crack propagation

The background of the simulation applied in this study is described in Ref. 2. The residual tangential stress σ_Θ and the radial stress σ_r in the matrix caused by the mismatch of the thermal expansion coefficients between matrix and particles are given by[6]

$$\sigma_\Theta = -\sigma_r = \sigma_i \frac{R^2}{r^2} \tag{1a}$$

$$\sigma_i = \frac{2\mu_1\mu_2[(1+\nu_2)\alpha_2 - (1+\nu_1)\alpha_1]\Delta T}{[\mu_1 + (1-2\nu_1)\theta_2]} \tag{1b}$$

where $\mu_{1,2}$, $\nu_{1,2}$ and $\alpha_{,1,2}$ are the shear modulus, Poisson's ratio and thermal expansion coefficients of the particle and the matrix, respectively. ΔT is the temperature difference between processing and room temperature, R is the radius of the particles, and r is the distance from the center of the particle. The stresses in the particles are hydrostatic and constant and can be calculated from eqn (1) by setting $r = R$.

The stress intensity factors at the crack tip under both residual and applied stress fields were computed numerically by the Body Force Method (BFM).[7] The BFM is a kind of simplified boundary element method, giving highly accurate solutions in a short time span, especially for a two-dimensional elastic problem. For the calculations of stress intensity factors by the BFM, the coordinates describing the geometrical shape of the corresponding crack and the applied loading condition are required as input-data. The applied stress intensity factor, K_a, and the residual stress intensity factor, K_r, were calculated separately and the total stress intensities for mode I and II at the crack tip, K_I and K_{II}, were obtained by superposition of both loading cases:

$$K_I = K_{Ir} + K_{Ia} \tag{2a}$$

$$K_{II} = K_{IIr} + K_{IIa} \tag{2b}$$

where K_a can be written as a function of the applied stress, σ_a, that is, $K_a = \sigma_a K'$. K' is the actual stress intensity factor at the deflected crack tip per unit applied stress under uniaxial tension.

The particles were replaced by pressurized voids of 16 edges, which has been shown to be a good approximation for values of $r > 1{\cdot}02R$. For values of $r < 1{\cdot}02R$, the errors in both stress distribution and K' become considerable. Therefore, an imaginary interface was modeled at $r = 1{\cdot}05R$, and cracks which impinge on the particles propagate along this imaginary interface. Residual stresses around the particles were calculated by using eqn (1), inserting reported values for $\mu_{1,2}$, $\nu_{1,2}$ and $\alpha_{1,2}$ and assuming 1200°C as the value of ΔT. These values are summarized in Table 1.

3 Results and Discussion

3.1 Mechanical properties

The mechanical properties of both the monolithic and the composite material are given in Table 2. Both materials can be considered as fully densified. Through the addition of particles, the bending strength decreased remarkably from about 500 to 316 MPa, whereas the fracture toughness increased considerably from 2·8 to 6·0 MPa$\sqrt{\text{m}}$.

Mechanisms that attribute to the observed increase in fracture toughness through the addition of 20 vol% alumina particles are crack deflection, crack pinning, and crack wake bridging.[8,9] These mechanisms are correlated with the residual stresses around the particles due to the mismatch between the thermal expansion coefficients of alumina and silicon carbide.

Table 1. Material properties of SiC and Al_2O_3

	SiC	*Al_2O_3*
Thermal expansion coefficient (°C^{-1})	$5{\cdot}12\times10^{-6}$	$8{\cdot}1\times10^{-6}$
Shear modulus μ (GPa)	180	162
Poisson's ratio ν	0·25	0·235

Table 2. Mechanical properties of SiC and SiC/Al_2O_3 $(20\,vol\%)_p$

	SiC	*SiC/Al_2O_3 $(20\,vol\%)_p$*
Relative density (%)	99·8	99·5
Bending strength σ_B (MPa)	495	316
Fracture toughness K_{IC} (MPa$\sqrt{m}$)	2·8	6·0

3.2 Crack propagation

Figure 1 shows an optical micrograph of a crack propagating from the edge of a Vickers indentation. It can be seen that the crack is repelled by the alumina particles due to the residual tensile stresses around the particles in radial direction. A composite material with distributed particles was modeled and crack propagation was simulated using the BFM. The results are shown in Fig. 2 Similar to the experimental crack propagation, the crack is deflected when it approaches a particle, in agreement with eqn (1).

3.3 Crack propagation through graded particle distributions

Crack paths and fracture resistance behavior were investigated by simulation for composites with graded particle distributions. The particles were introduced in the range of $0 < x/R < 18$ and $-7 < y/R < 7$, the crack starts to propagate from $x = -5R$ at $y = 0$. Graded particle distributions were configurated in two variations: in the first case, the number of particles per volume unit at the crack tip increased with crack propagation (Fig. 2); in the second case, the crack approaches a zone with a large number of particles, propagating into a zone without particles (Fig. 3) Both figures show the geometry of crack propagation as well as the normalized fracture resistance as a function of crack propagation.

In general, the fracture resistance increases when the crack approaches a particle due to the residual compressive stresses in tangential direction which are acting as a crack-closing mode. When the crack tip is located above or below a particle, as it should be generally the case, the residual tensile stresses in radial direction are prevailing, resulting in a remarkable decrease in fracture resistance. The stress state around the particles due to the mismatch between the thermal expansion coefficients according to eqn (1) is schematically illustrated in Fig. 4

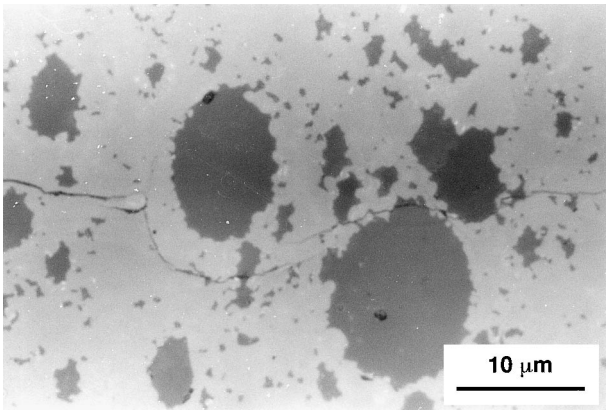

Fig. 1. Optical micrograph of a crack originating from the edge of a Vicker's indentation. The crack propagates from left to right in SiC/Al_2O_3 $(20\,vol\%)_p$.

In the case of randomly distributed particles without gradient, it has been reported by Kim *et al.* that the fracture resistance, K_{ca}, increases when the crack approaches the region of particle distribution and that it decreases below the matrix value K_{cm} when the crack enters the particle-region. This has been explained with the prevailing of crack-opening modes that emerges when the particles are located above or below the crack surface.

The fracture resistance values of Al_2O_3–SiC composite materials obtained by these simulations have been shown to exhibit remarkably lower values than experimental results would suggest. This contradiction has been explained by the characteristics of a 2D simulation.

Although the fracture resistance behavior which was observed in this work showed the same tendencies, characteristic differences have been found between the two graded materials.

In the case of increasing volume fraction of particles with crack advance, the normalized fracture resistance values remained on a level higher than 1 until the crack had to deflect around a particle (a). It may be expected that the residual tensile stresses in radial direction and the residual compressive stresses in tangential direction caused by these particles are superposed in a way that the resulting stress distribution enhances fracture resistance.

When the crack propagates along the interface of particle 4, the fracture resistance becomes zero. The residual tensile stresses in radial direction exhibit their maximal value at the interface, thus, the crack propagates easily. In many ceramic composites, the fracture toughness of the interface between matrix and particle is relatively low.

After passing particle 4, the crack changes its direction again and propagates horizontally. When approaching the next particle, the fracture resistance increases remarkably, exhibiting a maximum at $x/R = 10{\cdot}5$, where the crack reaches the interface of particle 5. When the crack propagates along the interface of particle 5, the fracture resistance drops to zero again. Instead of continuing to propagate horizontally, the crack is deflected by a cluster of particles in front of the actual position of the crack tip. This cluster seems to act similar as a large single particle, because the stress fields of

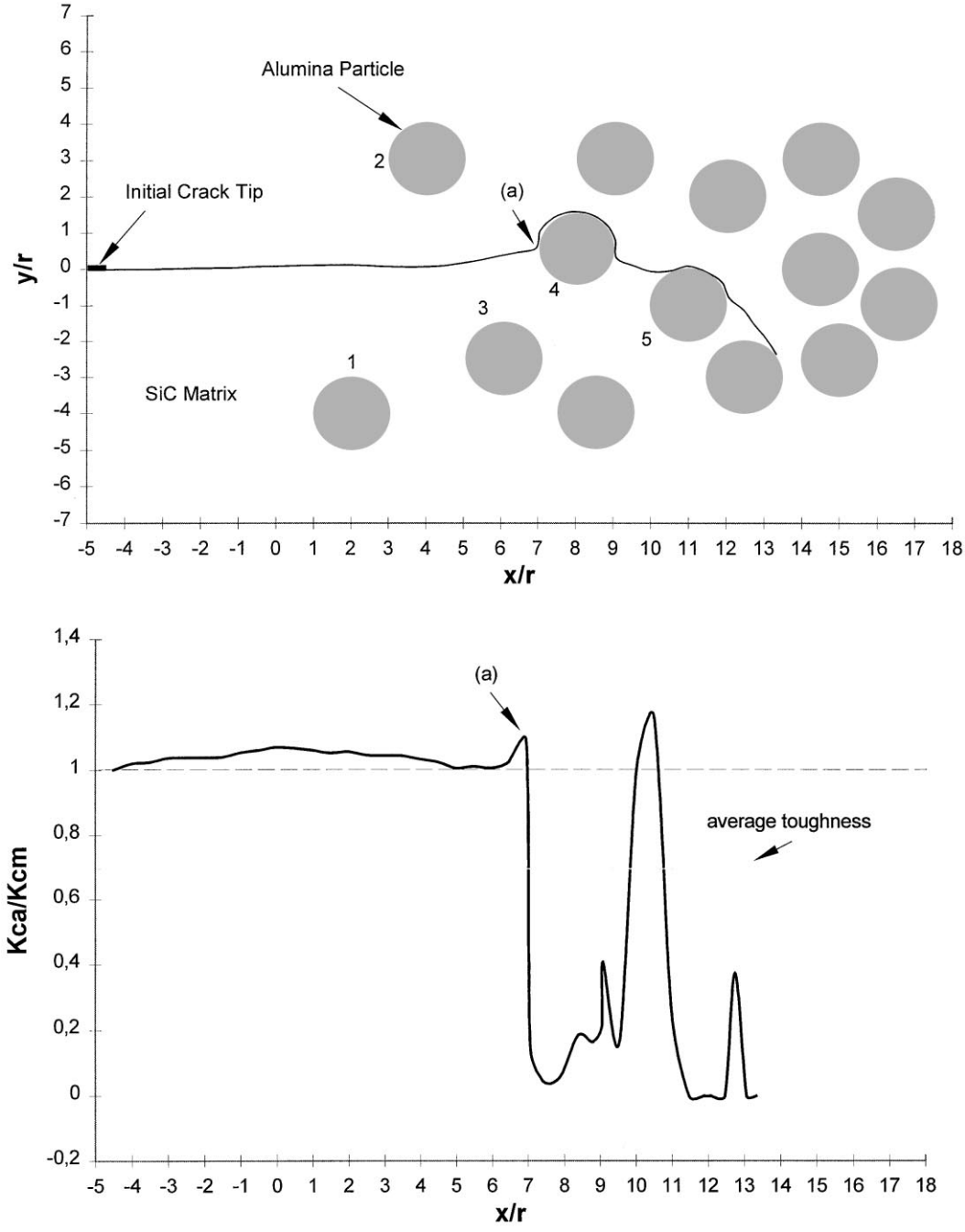

Fig. 2. Simulated crack path and related variation of apparent fracture resistance in SiC/Al_2O_3 $(20\,vol\%)_p$ with graded particle distribution. The crack propagates from left to right.

various particles are superposed, resulting in a crack path which is perpendicular to the residual tensile stresses of the particle cluster and thus the fracture resistance is remaining at a low level.

The same effect can be observed when the crack approaches a zone with a large number of particles, as it can be seen in Fig. 3. The crack is forced to leave its original direction by the superposed tensile stress fields of the particles in front of the crack tip. The superposed residual compressive stresses in tangential direction are resulting in an enhanced fracture resistance when the crack approaches the cluster. But when the crack is changing more and more in a vertical direction, where residual tensile stresses of the particle cluster and particle 1 in front of the crack tip are prevailing, the fracture resistance decreases.

When the crack finds its way to penetrate the cluster, the direction of the crack path becomes perpendicular to compressive residual stresses of particle 2 again, resulting in a short increase in fracture resistance, before the crack reaches the interface of the particle and the fracture resistance decreases.

The overall value of K_{ca} is lower than K_{cm} for both graded particle distributions although local values of K_{ca} sometimes exceed K_{cm}. Average toughness values of K_{ca} are given in Figs 2 and 3. For both particle distributions, the average toughness value is the same.

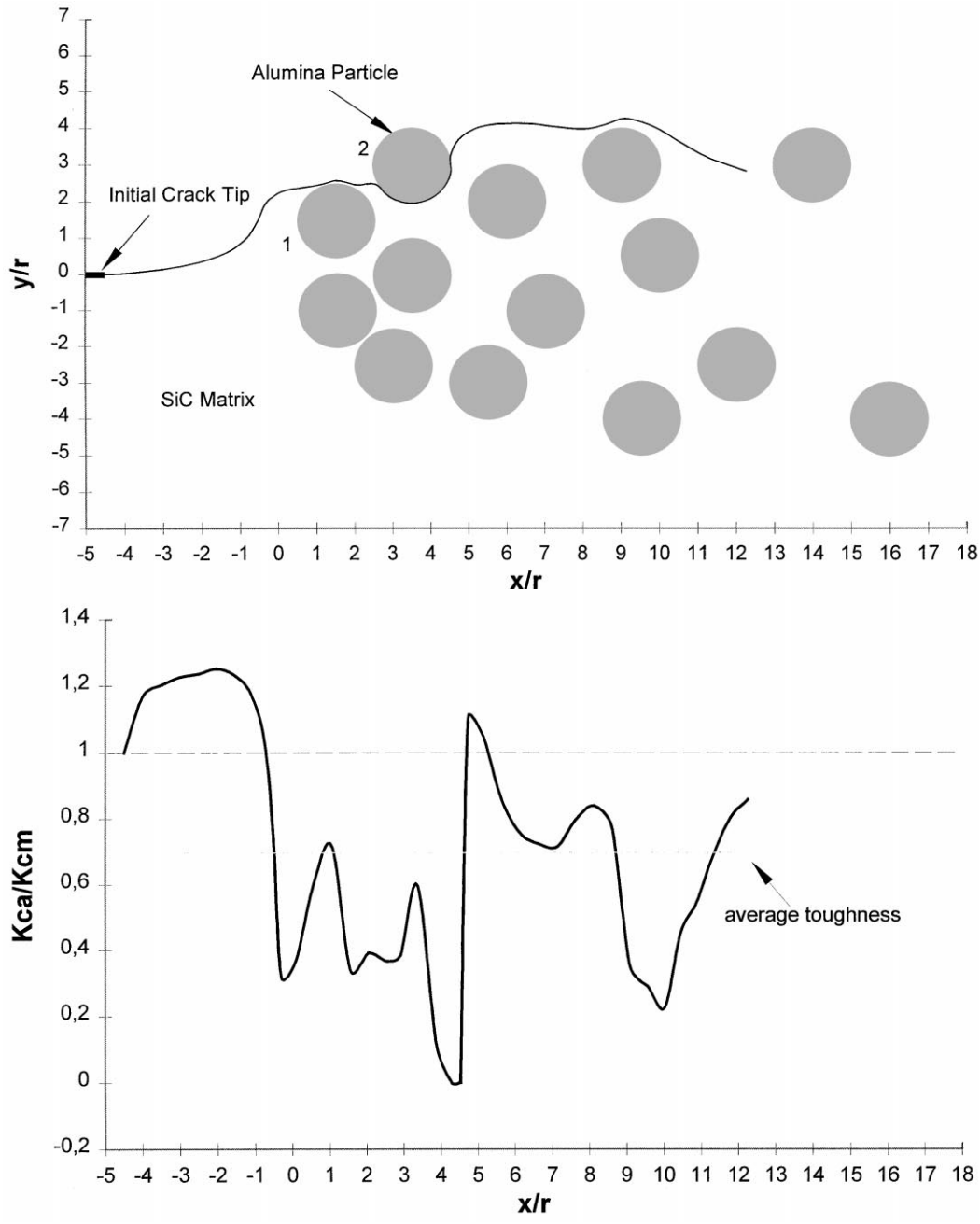

Fig. 3. Simulated crack path and related variation of apparent fracture resistance in SiC/Al_2O_3 $(20\,vol\%)_p$ with graded particle distribution. The crack propagates from left to right.

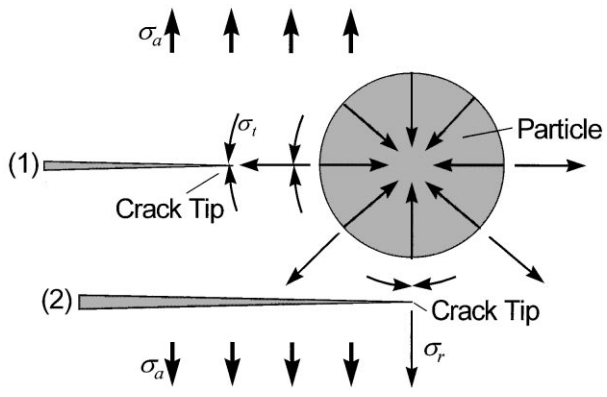

Fig. 4. Stress state around a particle with two crack tip positions: crack tip in front of the particle (1), where the residual compressive stress increases fracture resistance, and crack tip below the particle (2), where crack opening modes are prevailing.

The considerable increase in experimentally measured fracture toughness of SiC/Al_2O_3 composites can not be fully explained by the results obtained by the presented simulation. It is assumed that 3D-crack deflection contributes to enlarge the fracture surface, leading to a larger amount of fracture energy.

Other mechanisms which have not been considered in this simulation are microcrack toughening and crack wake bridging by debonded and partly pulled-out particles as well as crack wake bridging by matrix grains. The friction at the debonded surface of these bridges can contribute to enhance fracture toughness remarkably. Both bridging effects are correlated with the existence of residual stresses and crack deflection.

4 Conclusions

The fracture toughness of SiC could be increased through the addition of 20 vol% spherical alumina particles by a factor of 2. Experimentally observed crack paths in this composite material are similar to those obtained by simulation: Residual stress fields in the matrix due to the mismatch of thermal expansion coefficients are forcing the crack to deflect around particles. Residual tensile stresses in the radial direction of the particles are acting as a crack opening mode, residual compressive stresses in tangential direction contribute to close the crack. In graded particle distributions, the stress fields of the particles in densely populated areas superpose. When clustering occurs, the stress field around the cluster forces the crack to propagate around the cluster. Superposed residual stresses can result in local K_{ca} values higher than K_{cm}. In order to come to more realistic results as regards fracture toughness, it is supposed to consider 3D effects, microcracking and crack wake bridging in future considerations.

References

1. Kim, B.-N., Wakayama, S. and Kawahara, M. Characterization of 2-dimensional crack propagation behavior by simulation and analysis, *Int. J. Fract.*, 1996, **75**, 247–259.
2. Kim, B.-N., Watanabe, M., Enoki, M. and Kishi, T. Simulation of fracture behavior in particle-dispersed ceramic composites, *Eng. Fract. Mech.*, 1998, **59**, 285–303.
3. Nose, T. and Kubo, H., Toughening behavior of particle-dispersed ceramics. Proc. 3rd Japan International SAMPE Symposium, 7–10 December, 1993, p. 11–15.
4. Nandy, M.-O., Nose, T., Enoki, M. and Kishi, T. R-curve and cyclic fatigue behavior in alumina-particles-reinforced silicon carbide, *Mat. Transactions, Jap. Inst. of Metals*, 1996, **37**, 769–775.
5. Japanese Industrial Standards Committee, JISR 1607, 1990.
6. Yuuki, R., Xu, J.-Q. and Schmauder, S. Simple method to analyze the residual thermal stress of dissimilar materials and some applications, *Trans. Jpn. Soc. Mech. Eng.*, 1991, **A57**, 172–178.
7. Nisitani, H., Saimoto, A. and Noguchi, H. Versatile method of analysis of two-dimensional elastic problem by body force method, *Trans. Jpn. Soc. Mech. Eng.*, 1990, **A56**, 2123–2129.
8. Faber, K. T. and Evans, A. G. Crack deflection process – I. Theory, *Acta Metall.*, 1983, **31**, 565–576.
9. Swanson, P. L., Fairbanks, C. J., Lawn, B. R., Mai, Y. W. and Hockey, B. J. Crack-interface grain bridging as a fracture resistance mechanism in ceramics. I. Experimental study on alumina, *J. Am. Ceram. Soc.*, 1987, **70**, 279–289.